Luminescent Oil Soluble Carbon Dots Towards White Light Emission: A Spectroscopic Study

*Annamaria Panniello,[a] A. Evelyn Di Mauro[a], Elisabetta Fanizza,[a,b] Nicoletta Depalo [a] Angela Agostiano,[a,b] M. Lucia Curri,[a] Marinella Striccoli[a]**

[a] CNR-IPCF-Bari Division, c/o Chemistry Department, University of Bari "Aldo Moro", Via Orabona 4, 70126 Bari, Italy; b Chemistry Department, University of Bari "Aldo Moro", Via Orabona 4, 70126 Bari, Italy.

* m.striccoli@ba.ipcf.cnr.it

ABSTRACT Carbon dots (C-dots) are emerging as new emitting nanomaterials for optoelectronics, bioimaging and biosensing, thanks to their high quantum yield (QY), biocompatibility, low toxicity and cost effective sources. Although the origin of their photoluminescence (PL) mechanism (i.e. their strong blue-green emission and excitation dependent fluorescence) is still controversial, it has been demonstrated to depend on the synthetic protocols and experimental conditions, able to modify the surface properties. Here oil-dispersible C-dots, synthesized by carbonization of citric acid in the presence of hexadecylamine in high boiling organic solvent, are thoroughly investigated by systematically controlling the synthetic reaction parameters. Similarly to what found for water soluble C-dots, citric acid in the presence

of amine-containing passivating agents improves the PL emission of C-dots, *via* the formation of molecular fluorescent derivatives alongside the carbonization process. We demonstrate that, at growth temperature of 200°C, such C-dots exhibit an interesting and intense white emission, when excited in the blue region, thus resulting in a biocompatible colloidal white emitting single nano-objects. The incorporation of the nanoparticles in a poly(methylmethacrylate) (PMMA) host matrix, to obtain freestanding nanocomposite films, is demonstrated not to affect the colour point, that still falls in the white colour region of the 1931 CIE diagram. Remarkably, the emission properties are retained even after several months of films exposure to air and sunlight, thus confirming the colour stability of the nanoparticles against ageing.

1. INTRODUCTION

Recently, carbon nanodots (C-dots) have emerged as an effective alternative to the classical inorganic semiconductor quantum dots (QDs) for a wide range of applications, comprising sensors, photovoltaics, catalysis, bioimaging, drug delivery and optoelectronics. Compared to QDs, C-dots combine an intense and tunable photoluminescence (PL) with good biocompatibility, low toxicity, high resistance to photo-bleaching and inexpensive cost.[1]

Since their discovery, extensive efforts have been devoted to developing novel and original synthetic approaches and understanding the electronic and physical-chemical properties of the C-dots. In general, both top-down and bottom-up strategies have been exploited to prepare C-dots, offering the latter a wider choice of organic precursors and/or ligand molecules and diverse carbonization conditions.[1-3] Currently, several methods have been proposed to obtain water-dispersible C-dots, being generally based on hydrothermal reactions between an organic precursor bringing carboxylic moieties as carbon source, typically citric acid (CA), and a variety of amines

(e.g. ethanol-amine, ethylendiamine) as nitrogen source and surface passivating agents. The formation of the C-dots has been generally described as a sequence of steps denoted as poly-condensation and thermal pyrolysis or carbonization. The first step has been reported to produce amide derivatives generated from reaction between the carboxylic and amine groups that upon carbonization induce the formation of water-dispersible and highly emitting C-dots. Although quite simple, the water phase strategies suffer from the undesired formation of larger carbon structures induced by the hydrophilic surface functional groups as aggregation sites, and the resulting very broad size distribution requires post-synthetic purification (by means of filtration, dialysis, centrifugation, column chromatography and gel electrophoresis) to narrow the size distribution of C-dots and thus improving their properties.[4-5] Meanwhile, the hydrophilicity of such C-dots hinders their use in some specific applications, such as the fabrication of LEDs or optoelectronic devices and sensors, vulnerable to water exposure. Conversely, attracting perspectives can be offered by the synthesis of oil-soluble C-dots,[6-8] able to provide a precise control on size and emission, with a high QY. However, since one of the first synthesis proposed by Liu and co-authors,[9] only few studies have reported the preparation of C-dots in non-coordinating high boiling point organic solvents.[6-8] The mechanism proposed by Liu and co-authors[9] relies on a hot-injection approach, similar to that used for colloidal inorganic QDs. Highly luminescent oil-soluble C-dots have been prepared by quickly injecting anhydrous CA as carbon source into a heated mixture of octadecene (ODE) and 1-hexadecylamine (HDA), acting as non-coordinating solvent and surface passivating agent, respectively. This simple synthetic approach results in C-dots with multicolored PL emission, high luminescence efficiency optical properties dependent on reaction time. The reproducibility of this synthetic strategy facilitates fundamental studies and practical application of these oil soluble C-dots.

The still debated origin and nature of C-dot optical properties and PL emission, in particular, have inspired a number of studies[10-14] since the deep and comprehensive understanding of the fluorescence mechanisms is decisive to fully exploit their potential for technological applications. A general consensus from various reports highlights two main contributions to the radiative emission of C-dots whose intensity and peak position depend on the excitation wavelength: i) a contribution from the intrinsic carbogenic core, consisting of sp^2 domains and ii) a contribution deriving from the surface states, i.e. emission traps, surface defects, functional groups at C-dot surface.[13, 15-17]

Also, in hydrothermal synthesis it has been demonstrated that the use of CA, or similar compounds, as carbon source and the concomitant addition of amines induces an enhancement of the luminescence of the prepared nanoparticles (NPs), irrespectively from the synthetic parameters. As an example, an increased PL QY has been detected for water-soluble C-dots obtained by hydrothermal treatment of CA in the presence of amines, which has been reasonably ascribed to the formation of amide-containing molecular fluorophores during the precursor poly-condensation through heating.[15] Molecular fluorescent species can be formed in parallel alongside carbonization, and can notably influence the optical properties of the reaction products. Yang and co-workers[18] isolated, by separation and purification from the reaction mixture, an organic fluorescent derivative, the imidazo[1,2-α]pyridine-7-carboxylic acid, 1,2,3,5-tetrahydro-5-oxo-, IPCA, formed during the hydrothermal synthesis of C-dots from CA with ethylenediamine at 140°C for 10 h. Interestingly, the optical properties of such a fluorophore well match the absorption and emission properties of core and edge states of C-dots, with its QY (nearly 86%) considerably higher than that of the carbon states and its PL characteristic almost independent from the excitation wavelength. Similarly, in a recent paper, Rogach et al.[10] studied the synthesis of

different samples of C-dots obtained by the hydrothermal reaction at 200°C for 5h of CA with three amine ligands. The optical properties of the collected products have been compared with those of citrazinic acid, firstly recognized in 1884 as the most basic blue florescent molecule, presumably forming alongside the carbonization reaction of CA and amines, thus confirming the contribution of such a molecular unit on the emission properties of the as synthesized C-dots. These studies emphasize that when CA is used as carbon source in the presence of primary bifunctional or easily decomposing amines such as ethylenediamine or hexamethylene-tetramine, fluorescent molecules are formed, such as IPCA or citrazinic acid, respectively, mainly connected to the carbon core, and strongly contributing to the optical properties of the C-dots. Conversely, tertiary amines such as ethanolamine cannot induce the formation of such amide based fluorophore.

Here the synthesis of oil soluble C-dots prepared by carbonization of CA precursor in hot coordinating solvent[9] in the presence of hexadecylamine (HDA) has been investigated. We chose to take advantage of the tunability and reproducibility of this synthetic procedure, which is less extensively investigated compared to the more popular water phase strategies, to get insights in the composition, temporal and temperature dependent- chemical structures and optical properties of the as-synthesized C-dots. A comprehensive and systematic physical chemical study has been performed to evaluate the effect of the synthetic parameters on the optical characteristics of the resulting nanostructures. The influence of HDA, reaction time and temperature on the UV-Vis absorption and excitation-dependent PL emission and QY have indicated that, at lower reaction temperature, carbonization extent is low, while highly emissive molecular structures or aggregates arising from CA and HDA condensation appear to have a dominant effect on the absorption and emission spectra and QYs. In this case, two emission bands contribute to the fluorescence for

excitation in the range between 390 to 410 nm, that, remarkably, results in an overall intense emission in the white region, according to CIE 1931. This interesting outcome meets the technological requirement and interest devoted to the design of white emitting materials based on NPs and nanocrystals. It is worth to note that the white emission in nanostructured materials is often obtained by mixing semiconductor nanocrystals or fluorophores with complementary emission, which increases the complexity of the fabrication processes,[19-21] or by using single "magic-size" CdSe QDs,[22] limited in their practical application due to the toxicity Cd-heavy metal [23-25] . Here we demonstrated that white emission is obtained from single C-dots purposely synthesized by playing with the growth parameters. Such NPs have great potential as emitting components in the fabrication of safe white emitting diodes (white LEDs), offering a sustainable alternative to inorganic nanocrystals.[6, 26-29]

Subsequently, the oil-soluble C-dots have been easily incorporated in an organic poly(methylmethacrylate) (PMMA) host matrix resulting in a nanocomposite fabricated as freestanding solid film. The intense white emission is retained in the polymer matrix, ruling out any detrimental effect on the original C-dot fluorescence due to their interaction with the organic host.

Overall, the obtained results confirm the relevance of the proposed synthetic strategy not only for fundamental study on PL mechanisms of oil-soluble C-dots, but also the high versatility and plain processability of as-synthesized samples and their great technological potential in the realization of optoelectronic and photonic devices.

2. EXPERIMENTAL SECTION

2.1 Chemicals. All chemicals were used as received, without any further purification or distillation. Anhydrous citric acid, CA (≥ 97%), octadecene, ODE (90%), were purchased by

Aldrich. 1-Hexadecylamine, HDA (98%) was purchased by Fluka. All solvent used were of analytical grade and purchased from Aldrich.

Poly(methyl methacrylate), PMMA, with high MW, was purchased by BDH Chemicals LTD 29774.

2.2 Synthesis of C-dots. C-dots were synthesized by the thermal carbonization of CA as organic precursor, in non-coordinating solvent (ODE), in the presence of HDA as coordinating agent.[9] All the preparative steps were performed under nitrogen atmosphere using a Schlenk line, and starting from dried and degassed reactants.

In a typical synthesis, a variable amount (0.8 or 1.5 g) of HDA was dissolved in 35 mL of ODE under vacuum at 110°C for 30 min. Then, the mixture was heated at T>153°C under nitrogen flux, and 1 g of CA was quickly injected into the reaction flask under vigorous stirring, at temperature ranging from 200 and 300°C. The heating was kept at that temperature for the desired time. At the end of the reaction, the resulting solution was cooled at room temperature, and C-dots were purified by washing with acetone several times. The resulting C-dots were dispersed in common weakly polar solvents, such as chloroform or toluene.

2.3 C-dot/PMMA nanocomposite preparation. C-dot/PMMA nanocomposites were prepared by adding a proper amount (0.175 g) of C-dots to a solution of PMMA in chloroform (0.1 g/mL). The mixture was let under mechanical stirring until a homogeneous dispersion of C-dots in PMMA matrix was achieved. Freestanding films of C-dots in PMMA were then obtained by drop casting 50 µL of the chloroform nanocomposite dispersion onto a properly cleaned glass substrate, and removing the resulting film after the complete evaporation of the solvent.

2.4 Spectroscopic investigation. Attenuated Total Reflection Fourier Transform Infrared (ATR-FTIR) spectra were recorded by means of a PerkinElmer Spectrum One Fourier Transform

Infrared spectrometer equipped with both a deuterated triglycine sulfate detector and a three-bounce, 4 mm diameter diamond microprism as internal reflection element. The resolution was 4 cm^{-1}. The measurements were performed by dropping aliquots (3–5 μl) of the chloroform solutions of the C-dots, directly onto the upper face of the diamond crystal and the spectra were acquired upon solvent evaporation.

UV-Vis absorption spectra were recorded with a Cary 5000 (Varian) UV/Vis/NIR spectrophotometer. PL spectra were recorded by using a Fluorolog 3 spectrofluorimeter (HORIBA Jobin-Yvon), equipped with double grating excitation and emission monochromators. All optical measurements were performed at room temperature on samples obtained directly from synthesis without any size sorting treatment.

TR-PL measurements were performed by Time-Correlated Single Photon Counting (TCSPC) technique, with a FluoroHub (HORIBA Jobin-Yvon). The samples were excited at 375 nm by a picosecond laser diode (NanoLED 375L) emitting $\tau \approx 80$ ps pulses at a 1 MHz repetition rate. The PL signals were dispersed by a double grating monochromator and detected by a picosecond photon counter (TBX ps Photon Detection Module, HORIBA Jobin-Yvon). The temporal resolution of the experimental set up was ~200 ps.

The emission quantum yields and 1931 CIE color point measurements of both solution and solid samples were obtained by means of a ‘‘Quanta-phi’’ integrating sphere coated with Spectralons and mounted in the optical path of the spectrofluorometer, using as an excitation source a 450 W xenon lamp coupled with a double-grating monochromator.

2.5 Morphological investigation. Transmission electron microscopy (TEM) imaging was carried out using a JEOL JEM1011 microscope, operating at an accelerating voltage of 100 kV and equipped with a W electron source. The images were acquired using a Gatan Orius

SC1000CCD camera. C-dots were deposited by drop casting onto TEM carbon-coated copper grids. The statistical analysis of the samples was performed by use of a freeware image analysis program. In particular, the average NP size and the percentage relative standard deviation (s%) were calculated for each sample to get information on the NPs size distribution.

3. RESULTS AND DISCUSSION

Luminescent C-dots have been synthesized by a one-step procedure similar to the one reported previously by Liu et al.[9] consisting in the carbonization of anhydrous citric acid (CA) as precursor, carried out in a mixture of octadecene (ODE) and hexadecylamine (HDA) as non-coordinating solvent and surface ligands. CA, which is abundant in nature, has been chosen as carbon source, since it represents an important starting material for the bottom-up synthesis of C-dots, being involved in fluorescent derivatives that strongly contribute to improve the QY. It may form chemical structures that can evolve from small fluorescent molecules, such as citrazinic acid derivatives, generated from the intramolecular condensation of CA with amines, to polymer clusters and carbon cores alongside carbonization.

Here, the synthetic conditions have been systematically varied to assess the role of the preparative parameters, namely (i) capping agent concentration, (ii) reaction time and (iii) temperature on the optical and morphological properties of the resulting NPs. UV-Vis absorption and excitation dependent emission and QY values have been investigated to get insights in the optical properties and chemical structures of the as-synthesized C-dots.

3.1 The role of the capping agents.

Three C-dot batches have been synthesized by injecting 1 g of CA at 250°C in the reaction mixture without HDA (“bare C-dot") and with 0.8 and 1.5 g of HDA (“HDA-added C-dots”),

setting the reaction growth temperature at 300°C and reaction time at 30 minutes. The TEM investigation, performed after reaction mixture purification, reported in Figure 1 (a-c), shows small dark spots less than 5 nm ascribed to C-dots with a spherical shape, whose size is not significantly affected by the amount of added HDA (Figure 1 a-b)

FT-IR measurements (Figure 1d-e) have been performed, which generally provide information on the functional groups of the nanostructures,[30] and here is useful to predict their chemical structures of the as-synthesized type of C-dots. FT-IR spectrum (Figure 1d) of C-dots synthesized in the presence of HDA (irrespectively of the HDA amount added) shows a sharp peak at 1690 cm^{-1}, ascribed to the amide carbonyl stretching vibration, probing that carbonyl groups of the CA were converted into amide group during the synthesis.[20, 31-32]

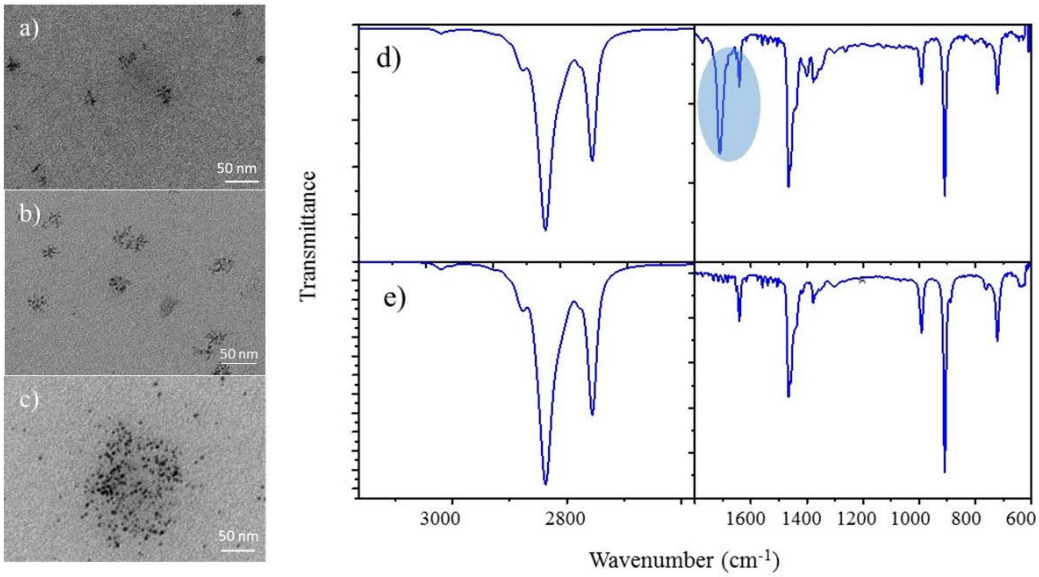

Figure 1. TEM micrographs (a, b, c) and FTIR spectra (d, e) of C-dots samples prepared with HDA 1.5 g (a, d) and 0.8 g (b) and bare C-dots (c, e).

Being completely absent in the bare C-dots sample, we can undoubtedly confirm that under the synthetic conditions, amide structures were formed thanks to conjugation between primary amine HDA and carboxylic groups of CA.

UV-vis absorbance spectra of all the three batches of C-dots show an intense absorption in the UV region, below 300 nm (Figure 2a), with an evident, broad peak at around 350 nm for HDA-added C-dots. Such a band becomes more intense and symmetric as the HDA amount added to the reaction increases from 0.8 g to 1.5 g, with a concomitant appearance of an absorption tail at lower energies, at wavelength longer than 400 nm.

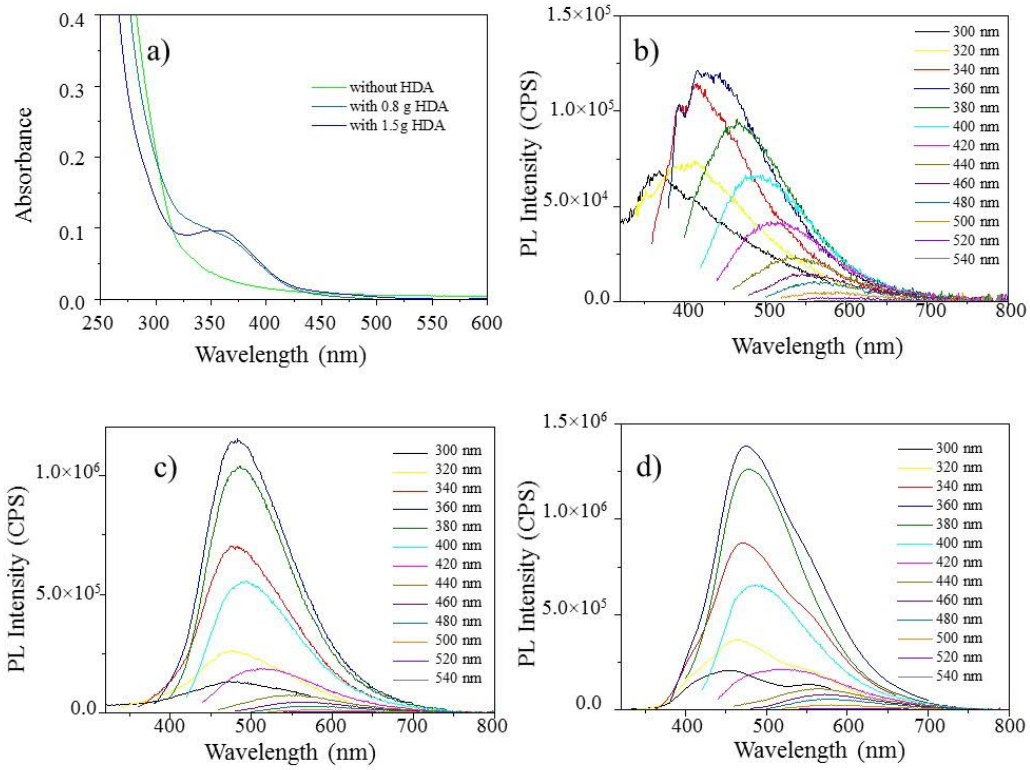

Figure 2. (a) UV-vis absorption spectra of chloroform dispersion of C-dots synthesized without (green line) or with (blue and cyan line) hexadecylamine (HDA) capping agent. PL spectra of chloroform dispersion of C-dots synthesized without HDA (b), and in the presence of 0.8 g (c) and 1.5 g (d) of HDA, respectively, recorded at increasing excitation wavelength.

As widely reported in literature, the intense absorption below 300 nm can be safely ascribed to the π-π* transition of the sp^2 domain originating by the conjugated C=C double bonds of the carbon core,[31-33] while the signal at 350 nm can be attributed to the n-π* transitions of the C=O bond of the carbonyl and of the amide functional groups at the C-dots surface, being only detected in HDA-added samples and completely absent in the absorption spectrum of bare C-dots. The extended absorption tail, above 400 nm, has been assigned to the surface state sub-bands absorbing at lower energy with respect to the n-π* transitions.[10] It is worth to note that, in spite of different reaction conditions, the absorption features of HDA added C-dots strongly resemble to those found by Rogach et al.[10] for hydrothermally synthesized water soluble C-dots, prepared by condensation of CA and ethylendiamine. In that case the high absorption below 300 nm, generally ascribed to the carbogenic core, was attributed also to π-π* transitions of the molecular fluorophores formed during carbonization process as citrazinic acid or its derivatives, as IPCA. In addition, the broad peak around 340 nm was ascribed to n-π* transitions of organic fluorophores. Moreover, a recent investigation reveals that such an absorption band can be due to the twofold contribution of the n-π* transitions and π-π*charge transfer involving aggregation of surface or molecular states within or among the C-dots.[11]

Wide and asymmetric emission bands characterize the PL spectra of the three as synthesized C-dots samples reported in Figure 2b-d. Emission has been recorded at different excitation wavelengths in the range between 300-500 nm, in order to depict the contribution of the carbogenic core, surface related states and/or the organic fluorophores potentially forming during the reaction.[10, 18] It is worth to note that both carbon core and edge state emission result excitation dependent, while the emission of the fluorescent molecular derivatives is expected to be independent form the excitation wavelength. The trend of PL peak wavelength versus excitation

wavelength in Figure 3a clearly indicates a tight dependence of the emission peak from the excitation for both the bare C-dots (green line in Figure 3a), and the HDA added C-dots (blue and cyan line in Figure 3a), irrespectively from the amount of HDA used during the reaction. However, while for the bare C dots, the PL peak centered at 367 nm for λ_{ex} of 300 nm, continuously red shifts by increasing excitation wavelength, the HDA added C-dots show a PL peak, whose position remains almost unchanged at nearly 470 nm for λ_{ex}< 400 nm, and slightly moves to higher value by increasing excitation wavelength up to 582 nm for λ_{ex}=500 nm. Moreover, the PL intensity versus excitation wavelength reported in Figure 3-b shows a strong excitation dependent PL intensity for syntheses carried out in presence of HDA, with the highest emission value obtained at λ_{exc} of 360 nm.

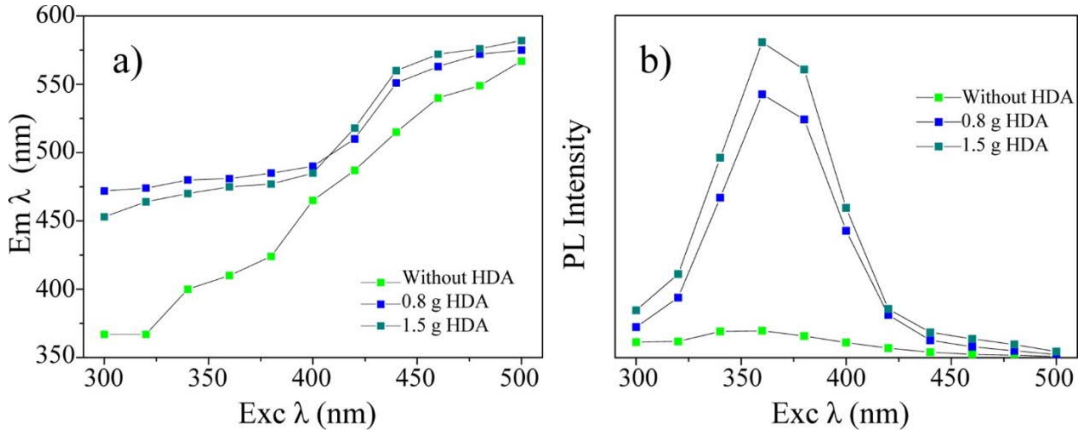

Figure 3. PL peak position (a) and PL intensity (b) as a function of the excitation wavelength for the bare C-dots (green symbols), and for the C-dots synthesized in the presence of 0.8 and 1.5 g of HDA (blue and light blue symbols, respectively).

This trend is in agreement with the absolute PL QY values reported in Table S1: PL QY of bare C-dots has a constant and low (nearly 1) value, irrespectively from the excitation wavelength, while HDA added C-dots show PL QY between 10 and 20% for excitation wavelength below 400 nm. This value drops down to 3% for λ_{ex}= 420 nm. Comparing the emission properties of the

samples synthesized without and with HDA suggests the contribution of different emission process (i.e emission states or emitting species) to the PL behavior.

The observed emission features of oil-soluble C-dots are very similar to what reported in the hydrothermal synthesis of water soluble C-dots carried out in the presence of amines.[10] In that case, the detected fluorescence was attributed to the formation of derivatives of citrazinic acid and to surface states, in the high (<400 nm) and low energy range, respectively.[10] As a molecular fluorophore, the citrazinic acid has a PL peak that does not change in position (PL peak at nearly 440 nm) with excitation wavelength and has higher PL intensity below 400 nm. In our case, although the fluorescence cannot be univocally assigned to the occurrence of a specific fluorophore, it can be safely inferred that most HDA or amino terminated molecules in the synthesis may induce, through the poly-condensation with carboxylic precursors, the formation of highly emissive fluorophores that can be accounted for the excitation-independent (for λ_{ex} below 400 nm) behavior of C-dots prepared in the presence of HDA and to the high PL QY value.[34-35] Blank experiment carried out by heating at 300°C for 30 min (and even prolonged time) the reaction mixture based on 1.5 g HDA in ODE without CA has been also carried out. The spectroscopic characterization (See Supporting Information Figure S1) reveals absorption and emission features matching well those of the bare C-dots, with a very low emission intensity. Therefore, we can undoubtedly assume that the PL of the oil-soluble, HDA added C-dots can be mostly originated from molecular states (i.e. IPCA and the citrazinic acid derivatives[10, 18]), formed during the synthesis when both CA and HDA are present in the reaction flask, arising from the condensation of CA carboxylic moieties and amines groups of HDA. Moreover, such blank experiments allow for highlighting the heterogeneity of the contribution from both carbon core nanoparticles and fluorophores, as reported in Kumbhakar *et al.*[36-37].

To gain information on the recombination dynamics, a time resolved (TR) emission study has been carried out by using a time-correlated single-photon counting (TCSPC) system. The PL decay of bare and HDA added C-dots has been probed at 435 nm, corresponding to the PL maximum, and are reported in Figure 4.

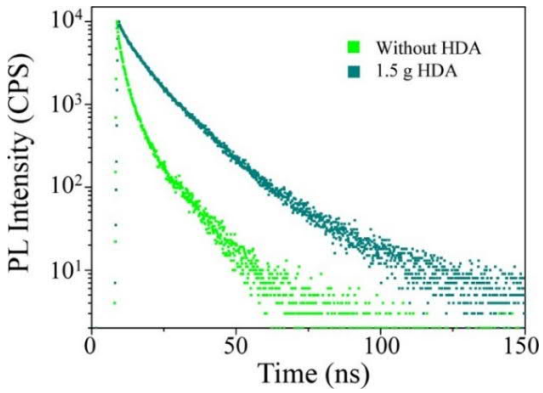

Figure 4. Comparison of time-resolved PL decays of $CHCl_3$ dispersions of bare C-dots and HDA-capped C-dots (1.5 g), exciting the solutions with a 80 picosecond pulsed light at 375 nm and detecting at 435 nm.

All the PL decay experimental data are best fitted by a bi-exponential function, although fitting ranging from mono-exponential to 4-exponential equations have been reported, depending on the synthetic procedure and on the surface properties of C-dots.[12, 17, 32, 34] The fitting parameters are reported in Table S2, where A1 and A2 are the pre-exponential factors, τ1 and τ2 the decay times. The average lifetime, τ_{Avg} has been calculated according to our previous study[38] _ENREF_33and reported in Table S2. The recombination dynamics of both the samples show a slow and a fast component, respectively. In bare C-dots, where the carbogenic core mostly contributes to the PL emission, the faster recombination is the dominant component of the decay. Conversely, in HDA-capped C-dots, the slower component prevails. Moreover, the average decay lifetime increases

passing from 4.6 to 12.2 ns for the bare C-dots and HDA-capped C-dots, respectively. The TR-PL measurements, together with the QY data, indicate that the presence of the coordinating agent promotes the formation of fluorophores that remarkably contribute to the radiative PL decay.

3.2 Effect of the reaction time

The reaction time has been varied while keeping unchanged the others synthetic conditions. In particular, 1.5 g of HDA have been added to the high boiling solvent (ODE) in the reaction flask and after the injection at 250°C of 1 g of the CA precursor, the reaction mixture has been heated at 300°C for 8, 30 and 180 minutes, respectively. The temporal evolution of absorption and PL characteristic versus reaction allows to consider the role of chemical composition and particle size on the optical properties of the formed C-dots.

Figure 5a reports the UV-Vis spectra of chloroform dispersions of C-dots obtained at different reaction times. Increasing the reaction time from 8 to 30 and 180 minutes, the intensity of the absorption band at about 350 nm decreases (Figure 5a red, blue and black lines, respectively). After heating at 300°C for 180 min, only a slight shoulder remains in the same absorption region. (Figure 5a, black line).

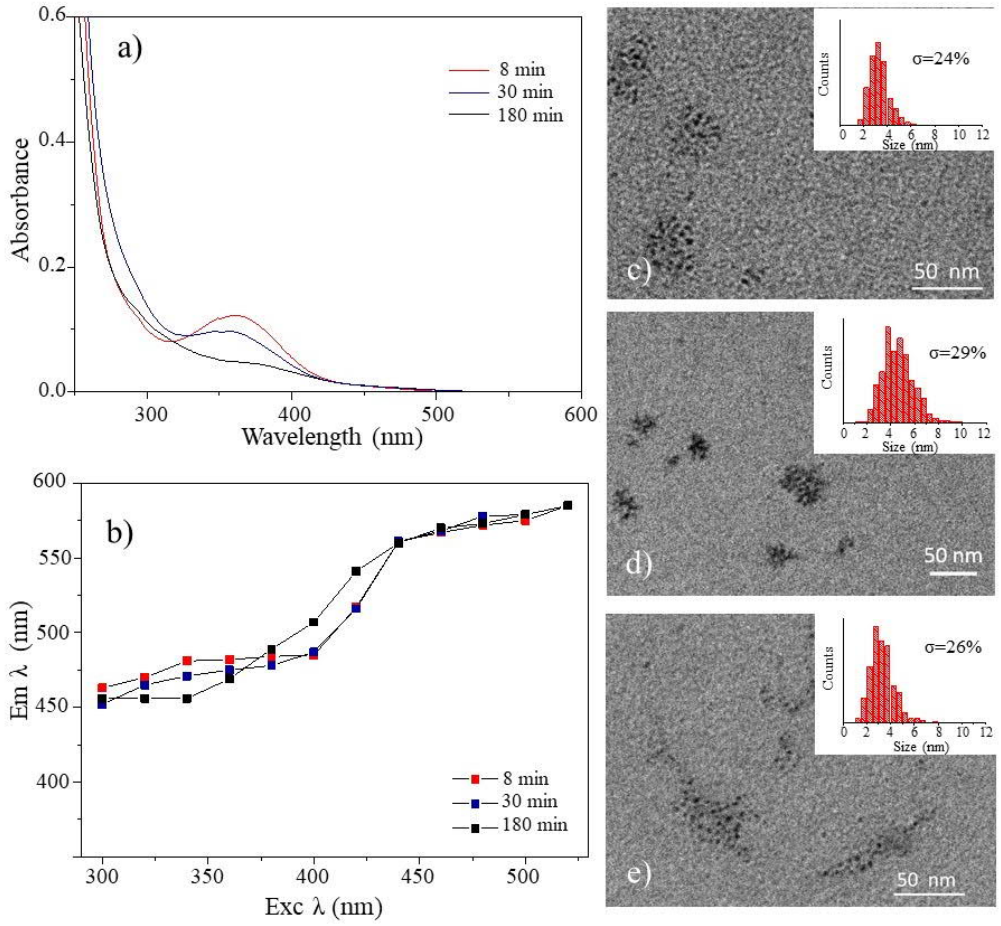

Figure 5. a) UV-vis absorption spectra and b) PL peak position as a function of the excitation wavelength of chloroform dispersion of C-dots carbonized at 300°C for 8, 30 and 180 min; TEM images of C-dots carbonized at 300°C for c) 8, d) 30 and e) 180 min.

TEM micrographs in Figure 5c-e, reveal that, with the reaction proceeding, only a slight modification in the average size (from 3 to 5 nm) and broadening of the size distribution of the spherical NPs can be observed up to 30 minutes of reaction, similarly to what reported by Liu et al.[9] However, at 180 min a slight focusing of the size distribution is measured (Figure 5 d-e). At different reaction time PL spectra show the typical wide asymmetric fluorescence band that bathochromically shifts with the excitation wavelength (Figure S2 A-C) over distinct regions.[10]

The emission wavelength versus excitation wavelength scattered plots reported in Figure 5b for the three samples show a quite similar trend for the samples prepared at the early stage of carbonization (Figure 5b red and blue symbols for 8 and 30 minutes reaction time respectively). Conversely, at longer reaction time (Figure 5b black symbols for 180 min reaction time), a more pronounced dependence of the PL peak position from the excitation is observed. Also PL intensity sensibly decreases, becoming half with respect to those measured for sample growth time of 30 minutes. These results suggest that, at the early stage of the reaction, molecular fluorophores (free or attached at the C-dots surface) will form alongside carbonization, contributing to the PL properties. However, as the carbonization reaction proceeds these fluorescent derivatives most likely decompose or degrade, becoming less influent in the C-dots PL properties.

Also, absolute PL QYs, measured (excitation wavelength at 360 nm) for all the three samples, provide a clear support for the PL data (Table S3), confirming the hypothesis of molecular fluorophores consumption or degradation during the ongoing of the carbonization reaction. The longer the reaction time, the lower the quantum efficiency, since upon disappearance of the molecular fluorophores the main contribution to the PL remains the less efficient carbon states (core and edge states).

The temporal evolution of the optical and morphological properties versus reaction time, indicates that two concomitant competitive processes can be considered: (i) progress in the carbonization may lead to the formation of carbogenic cores as dominant emissive species: (ii) during the pyrolytic process the molecular and surface states may be modified. Indeed, when the reaction is stopped at the early stage, right after the precursor injection, a large fraction of molecular fluorophores can form, leading to high QY values.

3.3 Effect of the reaction temperature

Finally, to further investigate the role of the carbonization process in the synthesis of the amino added C-dots, the effect of the reaction temperature has been also studied. In particular, the C-dot synthesis has been performed by keeping constant the CA and HDA amount (1 g and 1.5 g, respectively), and adding the precursor to the non-coordinating solvent heated at 200°C. The carbonization reaction has been carried out at different temperatures (200°C or 300°C), for 30 or 180 min.

UV-vis absorption spectra of samples are displayed in Figure 6. As stated before, at 300°C, regardless the reaction time, only a broad band around 350 nm and a strong absorption in the UV region are detected. Decreasing the growth temperature at 200°C, an additional absorption band at about 450 nm is observed, which becomes more intense at increasing reaction time. According to a recent study,[11] the occurrence of such characteristic absorption band can be explained taking into account the possible occurrence of aggregates starting from the molecular fluorophores, resulting in absorption at lower energies. In this regard, FT-IR analysis do not show any significant variation in vibrational signals of C-dots grown at 200°C with respect to the other HDA-capped C-dots heated at higher temperature (data not reported).

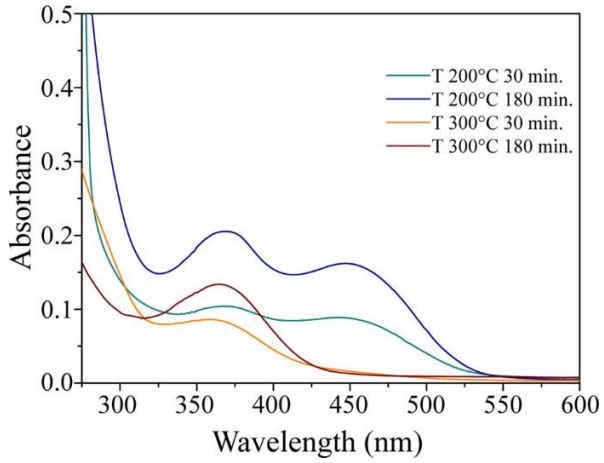

Figure 6. UV-vis absorption spectra of chloroform dispersion of C-dots as a function of the reaction temperature at two different reaction times.

The emission spectra of C-dots synthesized at 300°C, displaying a single broad emission band, are reported in Figure S3 A-B, while Figure 7 shows the emission spectra of C-dots grown at 200°C, for reaction time of 30 min (Figure 7a) and 180 min (Figure 7b), respectively. Interestingly, in this case the PL broad band results from the overlapping of two distinct contributions in spectral ranges centered approximately at 435 and 575 nm, respectively (Fig. 7 c-d) and their relative intensities modify with the excitation wavelength. At short λ_{Exc} the overall emission principally arises from the band centered at 435 nm.

At longer excitation (λ_{Exc}> 400 nm), the band centered at 575 nm becomes progressively stronger, while the band centered at 435nm decreases in intensity. For λ_{Exc}>420 nm (Figure 7a-b, purple line) the low energy band becomes the sole emissive contribution. A clear interrelation between this new emission state at lower energy and the appearance of an absorption feature at 450 nm for these types of samples, as reported in Figure 6, is out of debate. Figure 7 also compares the PL intensity (c) and the peak position (d) as a function of the excitation wavelength. The PL intensity shows the same trend of C-dots characterized by emission originating from both the

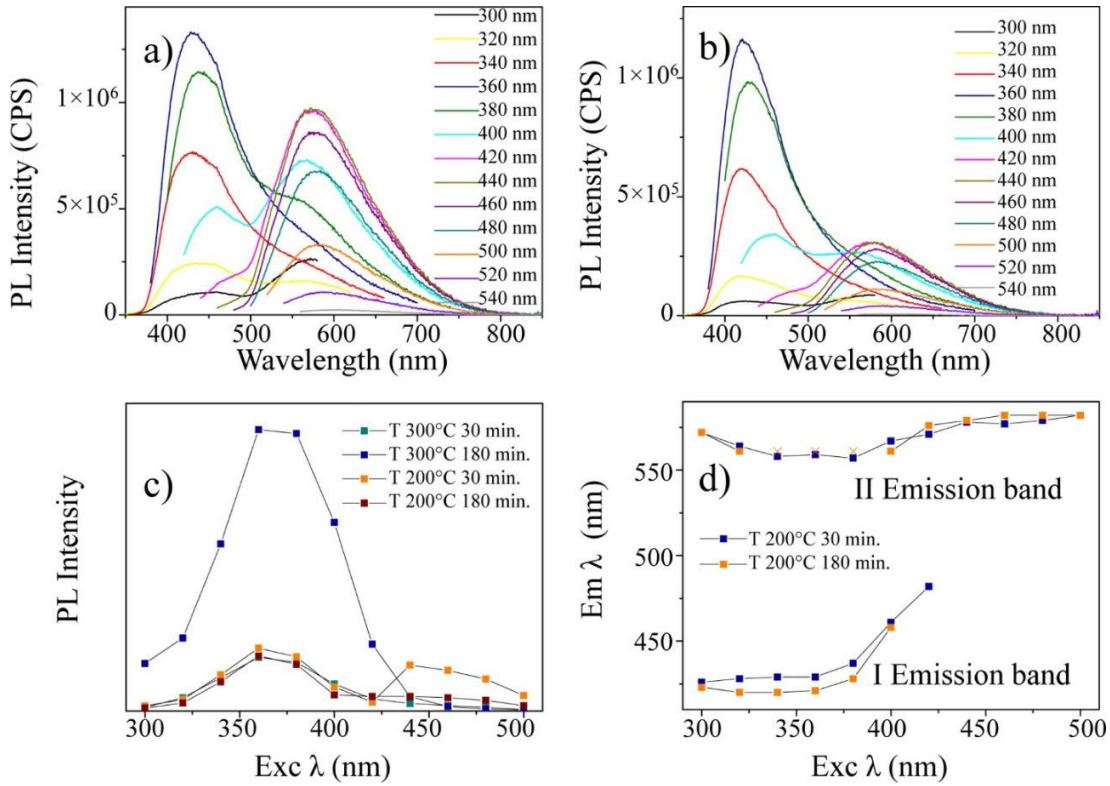

Figure 7. PL spectra of chloroform dispersion of C-dots grown at 200°C for 30 (a) and 180 (b) min, as a function of the excitation wavelength; (c) variation of PL intensity as a function of the excitation wavelength of C-dots grown at different temperatures and reaction times; PL peak position of the first and second emission band of C-dots synthesized at 200°C for 30 and 180 min.

molecular species and surface-related functional groups, as discussed before.[10] In addition, a pronounced emission tail is observed at excitation wavelength longer than 420 nm for samples grown at 200°C. Figure 7 b-c indicate, for the first emission band, a dependence from the λ_{Exc} in the range 360-420 nm for both the samples grown at 30 and 180 min. On the contrary, the peak of the second emission band only slightly shifts from its position, mainly when excitation wavelength is longer than 400 nm. Such second emission band can be considered due to the fluorescence of molecular species, being independent from excitation.[10] In particular, the progressive evolution towards red emissive states is consistent with the possible occurrence of aggregation among the

molecular fluorophores, whose absorption and emission signals are shifted to lower energies.[11] These overall evidences suggest a molecular origin of the emission at low energy.

The PLE spectra of sample grown at 300°C and performed in correspondence of the maximum PL emission at 435 and 575 nm show an intense excitation band, corresponding to the absorption transitions centered at 350 nm, a broad contribution at higher wavelength and a weak shoulder at 270 nm (Fig. 8-a). Conversely, for samples grown at 200°C, an additional excitation band is observed in correspondence of the absorption shoulder at 450 nm (Fig. 8 b-c). It is worth to note that a peak at high energy is present also for longer reaction time. Then, when C-dots are synthesized at lower temperature, a second band arises in the absorption, excitation and emission spectra. The presence of this intense band significantly contributes to the overall quantum efficiency. Indeed, the QYs of samples grown at 200°C are much higher than those of C-dots grown at 300°C (Table S3), characterized by a single PL band, reaching the value of 42% for excitation at 360 nm for reaction time of 30 min. The result is in agreement with the work of Kriesmann et al[15], demonstrating that at reaction temperature lower than 230°C, the PL mechanism is principally due to the highly emissive fluorophores formed by the condensation reaction between the carboxylic moieties of the CA and the amino functionalities of the passivating agent. At higher temperature, the pyrolysis starts to form carbonaceous core, and in such experimental conditions, the PL properties are expected to arise from both intrinsic core domains and fluorophores, that can be present as either intermediates or interacting species at the surface of the C-dots. Surface states can contribute to the emission properties of C-dots according to the preparative conditions with a variety of complex excited states. Then, the reaction time and the heating temperature play a decisive role in tuning the C-dot optical properties. Indeed, as the reaction time proceeds and the temperature is increased, the carbonization process advances and the carbogenic core is formed at

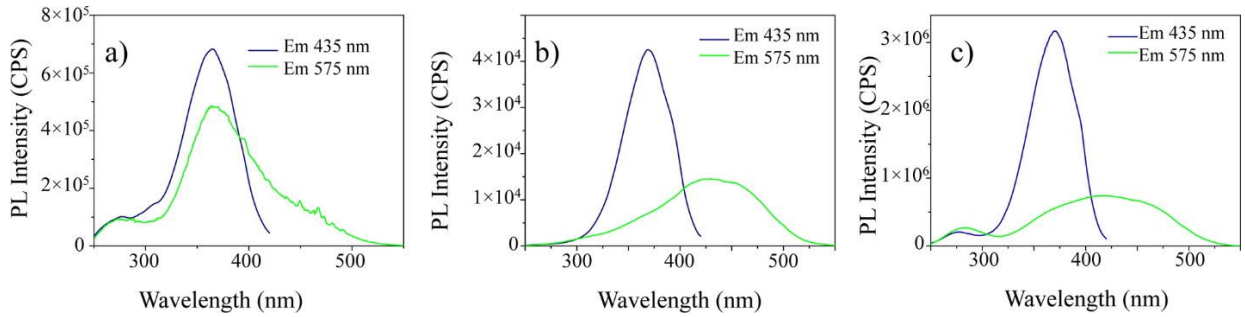

Figure 8. PL excitation spectra of chloroform dispersion of C-dots grown at 300°C for 30 min (a) or 200°C for 30 (b) or 180 min (c).

expenses of molecular species and surface connected functional groups, thus causing a decrease in QY, as already highlighted.

The presence of an additional band in absorption, excitation and emission spectra in the red region is indicative for the presence of multiple excited states emitting at low energies. Similarly to the findings of Kumbhakar et al.[11], although the different synthetic conditions, we can suppose the formation of complex aggregates of molecular fluorophores emitting at low energies that contribute to the overall PL emission of C-dots prepared in such specific synthetic conditions.

3.4 White PL emission

The synergistic effect of the carbogenic core and the molecular species and/or surface functional groups on C-dot optical properties accounts for intriguing implications arising from the multicolored emission of NPs showing the double emission band. Indeed, illuminating the chloroform dispersion of C-dots grown at 200°C by light of suitable wavelength, a white emission is observed. Figure 9-a shows the PL spectra of the C-dots grown at 200°C for 180 min by exciting at increasing wavelengths. For excitation from 390 to 410 nm, the PL emission broaden and cover almost the entire visible range of the spectrum, thanks to the enhanced contribution of the red component. In such conditions, when the C- dots are excited at 405 or 410 nm, they show an

intense white PL emission (inset of Figure 9-a). A similar behavior has been observed for C-dots grown at 200°C for 30 min (data not shown). The calculated CIE 1931 chromaticity coordinates in Fig. 9-b are (0.267, 0.315), (0.300, 0.361) corresponding to the excitation wavelength of 405 and 410 nm. Conventionally, “pure” white light is positioned as single point at (0.333, 0.333) coordinates in the CIE 1931 diagram. However, the white emission can be defined by

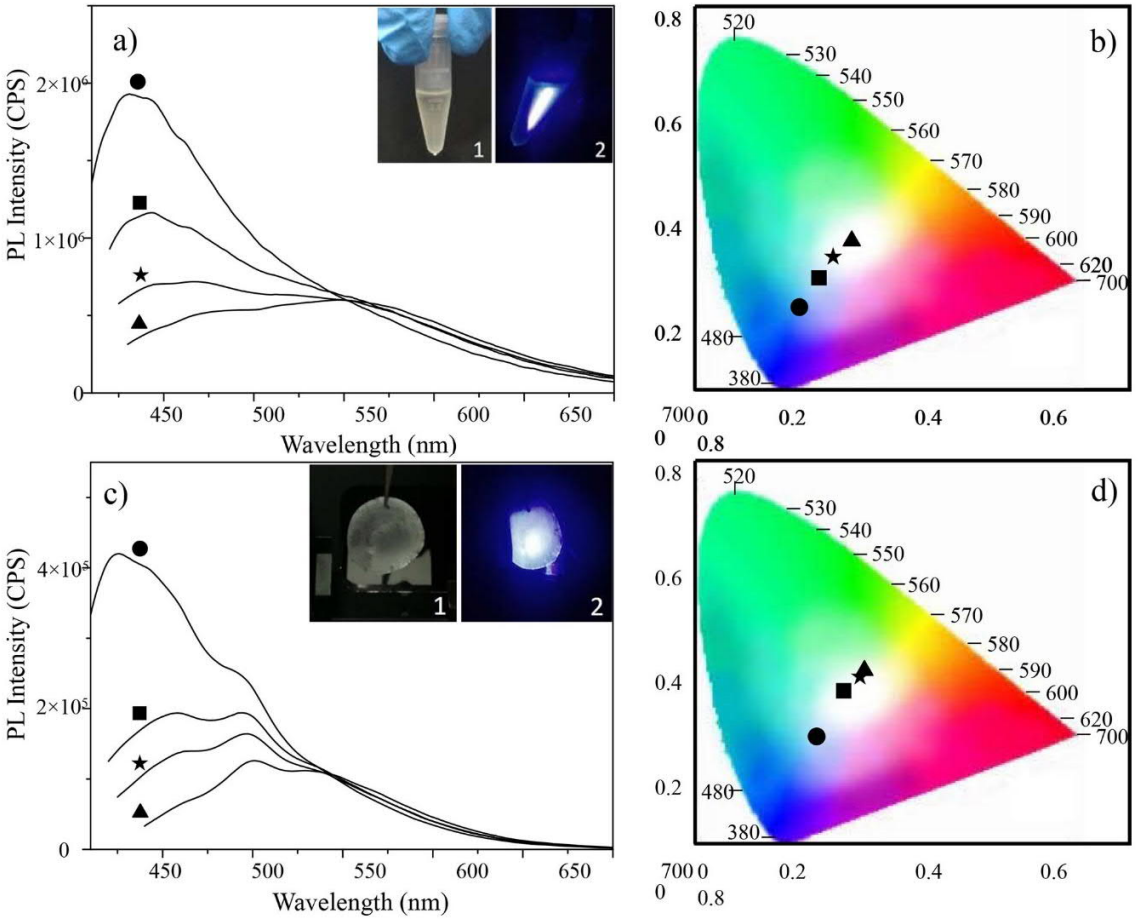

Figure 9. (a) and (c) PL emission spectra of C-dots in solution and film, incorporated in PMMA, obtained exciting at 390, 400, 405 or 410 nm (filled dot symbol, square symbol, star symbol or triangle symbol, respectively). In the insets, a picture of the vial and of the film under illumination with a laser diode at 405nm. (b) and (d) Position in the CIE 1931 diagram of C-dot dispersion and PMMA based film at the corresponding wavelengths.

complementary colors that properly combine, giving rise to a more extended white emission gamut.[39] Therefore, under illumination at 405 and 410 nm, the C-dot chloroform dispersion displays high PL emission in the white gamut (Inset of Fig. 9-a, and Fig.9-b), with QY of 24 and 22%, respectively.

Then, suitably playing with the synthetic parameters it is possible to prepare single carbon NPs characterized by an intense and stable white emission, being at the same time biocompatible, harmless and reasonably priced. The possibility to have such nano-objects disperse in organic solution and their high quantum efficiencies open the way to their successful exploitation in white light emitting devices.

In order to test the effective viability of the white emitting C-dots in practical applications, the as synthesized NPs have been simply incorporated into a suitable polymeric matrix, namely poly(methylmethacrylate), PMMA, to obtain nanocomposite solid films. Indeed, within the polymeric matrix, the C-dots can preserve or further enhance their optical properties taking advantage of the improved processability and mechanical properties of PMMA.[40]

PL emission spectra of the prepared nanocomposite films show the typical excitation dependent wide emission completely covering the visible spectrum (Figure 9-c). The PL emission consists of two main broad bands, contributing to the overall emission with intensities that depend on the excitation wavelength: the ratio between the underlying areas of the two contributing bands significantly changes with the increasing of λ_{Exc}. Upon incorporation in the polymeric matrix, the C-dots confirm the white light emission when excited at 400, 405 or 410 nm (Inset of fig. 9-c and Fig. 9-d). The coordinates of the CIE 1931 diagram of nanocomposite films are (0.291, 0.369), (0.319, 0.403), (0.335, 0.435) for excitation at 400, 405 and 410 nm, respectively (Fig. 9-d),

displaying high PL emission in the white gamut (Inset of Fig. 9-c, and Fig 9-d), with QY of 23, 20 and 18%, respectively.

In addition, the color stability in time of the white emitting C-dot/PMMA nanocomposite film has been tested by measuring the color point and the QY of the sample stored in air at room temperature, after several months of aging. The results (see Figure S4) show that the color point of the nanocomposite still falls in the white color region of the CIE 1931 diagram without substantial decrease of quantum efficiency (QY of 19% and 18% for excitation at 405 and 410 nm, respectively). The spectroscopic results indicate that upon incorporation of the C-dots in the organic matrix the emission features of the fabricated films are preserved, thus suggesting that the surface interactions with the host polymer do not affect the emissive states.

4. CONCLUSIONS

In summary, oil-soluble C-dots have been synthesized by a hot-injection method and systematically investigated by extensive physical and chemical characterization. Synthetic parameters as capping agent concentration, reaction time and temperature have been modified in order to evaluate their effect on the C-dot optical features. We have found that the presence of HDA, is fundamental in forming by poly-condensation both the amide bonds at C-dot surface and the intermediate molecular fluorophores that mostly contribute to the overall emission. Increasing reaction time and temperature advances the carbonization thus promoting the formation of carbogenic cores and the consumption of the molecular fluorophores, ultimately resulting in QY decrease. Interestingly, at lower reaction temperature, an additional absorption and emission band is observed. Irradiating such C-dots by visible light in the range 400-410 nm results in a bright fluorescence in the white gamut. Here, the proper choice of synthetic parameters allows for preparing functional materials with white emission based on biocompatible, harmless and low-

cost single carbon NPs. Their incorporation in a PMMA host matrix demonstrates the effective viability of such white emitting C-dots in practical applications. In particular, the polymeric matrix preserves the C-dot unique optical features and the nanocomposite solid films exhibit an intense white emission even after their storage in air at room temperature for several months.

ASSOCIATED CONTENT

Supporting Information. Partial characterization data, including PL spectra of C-dots at increasing reaction time, tables with QY values at different reaction conditions, table reporting the fitting parameters of the PL decays and the 1931 CIE diagram of the C-dot /PMMA film after aging

AUTHOR INFORMATION

Corresponding Author

* m.striccoli@ba.ipcf.cnr.it

Author Contributions

The manuscript was written through contributions of all authors. All authors have given approval to the final version of the manuscript.

Acknowledgments

This work was partially supported by the Bilateral Project CNR-CNRST Italy-Morocco 2016-2017, by the Apulia Region Funded Project NanoApulia (MDI6SR) and by the MIUR project PRIN 2015 (Prot. 2015XBZ5YA)

REFERENCES

1. Wang, Y.; Hu, A., Carbon Quantum Dots: Synthesis, Properties and Applications. *Journal of Materials Chemistry C* **2014**, *2*, 6921-6939.

2. Namdari, P.; Negahdari, B.; Eatemadi, A., Synthesis, Properties and Biomedical Applications of Carbon-Based Quantum Dots: An Updated Review. *Biomedicine & Pharmacotherapy* **2017**, *87*, 209-222.

3. Wang, R.; Lu, K.-Q.; Tang, Z.-R.; Xu, Y.-J., Recent Progress in Carbon Quantum Dots: Synthesis, Properties and Applications in Photocatalysis. *Journal of Materials Chemistry A* **2017**, *5*, 3717-3734.

4. Ding, H.; Yu, S.-B.; Wei, J.-S.; Xiong, H.-M., Full-Color Light-Emitting Carbon Dots with a Surface-State-Controlled Luminescence Mechanism. *ACS Nano* **2016**, *10*, 484-491.

5. Zhu, S.; Meng, Q.; Wang, L.; Zhang, J.; Song, Y.; Jin, H.; Zhang, K.; Sun, H.; Wang, H.; Yang, B., Highly Photoluminescent Carbon Dots for Multicolor Patterning, Sensors, and Bioimaging. *Angew. Chem. Int. Ed.* **2013**, *52*, 3953-3957.

6. Kim, T. H.; White, A. R.; Sirdaarta, J. P.; Ji, W.; Cock, I. E.; St. John, J.; Boyd, S. E.; Brown, C. L.; Li, Q., Yellow-Emitting Carbon Nanodots and Their Flexible and Transparent Films for White Leds. *ACS Appl. Mater. Interfaces* **2016**, *8*, 33102-33111.

7. Chung, W.; Jung, H.; Lee, C. H.; Kim, S. H., Extremely High Color Rendering White Light from Surface Passivated Carbon Dots and Zn-Doped Agins2 Nanocrystals. *Journal of Materials Chemistry C* **2014**, *2*, 4227-4232.

8. Bhunia, S. K.; Saha, A.; Maity, A. R.; Ray, S. C.; Jana, N. R., Carbon Nanoparticle-Based Fluorescent Bioimaging Probes. *Scientific Reports* **2013**, *3*, 1473.

9. Wang, F.; Pang, S.; Wang, L.; Li, Q.; Kreiter, M.; Liu, C.-y., One-Step Synthesis of Highly Luminescent Carbon Dots in Noncoordinating Solvents. *Chem. Mater.* **2010**, *22*, 4528-4530.

10. Schneider, J.; Reckmeier, C. J.; Xiong, Y.; von Seckendorff, M.; Susha, A. S.; Kasák, P.; Rogach, A. L., Molecular Fluorescence in Citric Acid-Based Carbon Dots. *J. Phys. Chem. C* **2017**, *121*, 2014-2022.

11. Sharma, A.; Gadly, T.; Neogy, S.; Ghosh, S. K.; Kumbhakar, M., Molecular Origin and Self-Assembly of Fluorescent Carbon Nanodots in Polar Solvents. *J. Phys. Chem. Lett.* **2017**, *8*, 1044-1052.

12. Shi, L.; Yang, J. H.; Zeng, H. B.; Chen, Y. M.; Yang, S. C.; Wu, C.; Zeng, H.; Yoshihito, O.; Zhang, Q., Carbon Dots with High Fluorescence Quantum Yield: The Fluorescence Originates from Organic Fluorophores. *Nanoscale* **2016**, *8*, 14374-14378.

13. Reckmeier, C. J.; Wang, Y.; Zboril, R.; Rogach, A. L., Influence of Doping and Temperature on Solvatochromic Shifts in Optical Spectra of Carbon Dots. *J. Phys. Chem. C* **2016**, *120*, 10591-10604.

14. Dhenadhayalan, N.; Lin, K.-C.; Suresh, R.; Ramamurthy, P., Unravelling the Multiple Emissive States in Citric-Acid-Derived Carbon Dots. *J. Phys. Chem. C* **2016**, *120*, 1252-1261.

15. Krysmann, M. J.; Kelarakis, A.; Dallas, P.; Giannelis, E. P., Formation Mechanism of Carbogenic Nanoparticles with Dual Photoluminescence Emission. *J. Am. Chem. Soc.* **2012**, *134*, 747-750.

16. Machado, C. E.; Tartuci, L. G.; de Fátima Gorgulho, H.; de Oliveira, L. F. C.; Bettini, J.; Pereira dos Santos, D.; Ferrari, J. L.; Schiavon, M. A., Influence of Inert and Oxidizing Atmospheres on the Physical and Optical Properties of Luminescent Carbon Dots Prepared through Pyrolysis of a Model Molecule. *Chem. Eur. J.* **2016**, *22*, 4556-4563.

17. Liu, X.; Pang, J.; Xu, F.; Zhang, X., Simple Approach to Synthesize Amino-Functionalized Carbon Dots by Carbonization of Chitosan. *Scientific Reports* **2016**, *6*, 31100.

18. Song, Y.; Zhu, S.; Zhang, S.; Fu, Y.; Wang, L.; Zhao, X.; Yang, B., Investigation from Chemical Structure to Photoluminescent Mechanism: A Type of Carbon Dots from the Pyrolysis of Citric Acid and an Amine. *Journal of Materials Chemistry C* **2015**, *3*, 5976-5984.

19. Jun, S.; Lee, J.; Jang, E., Highly Luminescent and Photostable Quantum Dot–Silica Monolith and Its Application to Light-Emitting Diodes. *ACS Nano* **2013**, *7*, 1472-1477.

20. Jang, E.; Jun, S.; Jang, H.; Lim, J.; Kim, B.; Kim, Y., White-Light-Emitting Diodes with Quantum Dot Color Converters for Display Backlights. *Adv. Mater.* **2010**, *22*, 3076-3080.

21. Woo, J. Y.; Kim, K.; Jeong, S.; Han, C.-S., Enhanced Photoluminance of Layered Quantum Dot–Phosphor Nanocomposites as Converting Materials for Light Emitting Diodes. *J. Phys. Chem. C* **2011**, *115*, 20945-20952.

22. Bowers, M. J.; McBride, J. R.; Rosenthal, S. J., White-Light Emission from Magic-Sized Cadmium Selenide Nanocrystals. *J. Am. Chem. Soc.* **2005**, *127*, 15378-15379.

23. Fanizza, E.; Urso, C.; Pinto, V.; Cardone, A.; Ragni, R.; Depalo, N.; Curri, M. L.; Agostiano, A.; Farinola, G. M.; Striccoli, M., Single White Light Emitting Hybrid

Nanoarchitectures Based on Functionalized Quantum Dots. *Journal of Materials Chemistry C* **2014**, *2*, 5286-5291.

24. Adam, M.; Erdem, T.; Stachowski, G. M.; Soran-Erdem, Z.; Lox, J. F. L.; Bauer, C.; Poppe, J.; Demir, H. V.; Gaponik, N.; Eychmüller, A., Implementation of High-Quality Warm-White Light-Emitting Diodes by a Model-Experimental Feedback Approach Using Quantum Dot–Salt Mixed Crystals. *ACS Appl. Mater. Interfaces* **2015**, *7*, 23364-23371.

25. Dai, Q.; Duty, C. E.; Hu, M. Z., Semiconductor-Nanocrystals-Based White Light-Emitting Diodes. *Small* **2010**, *6*, 1577-1588.

26. Chen, Y.; Zheng, M.; Xiao, Y.; Dong, H.; Zhang, H.; Zhuang, J.; Hu, H.; Lei, B.; Liu, Y., A Self-Quenching-Resistant Carbon-Dot Powder with Tunable Solid-State Fluorescence and Construction of Dual-Fluorescence Morphologies for White Light-Emission. *Adv. Mater.* **2016**, *28*, 312-318.

27. Joseph, J.; Anappara, A. A., White Light Emission of Carbon Dots by Creating Different Emissive Traps. *J. Lumin.* **2016**, *178*, 128-133.

28. Wang, Y.; Yin, Z.; Xie, Z.; Zhao, X.; Zhou, C.; Zhou, S.; Chen, P., Polysiloxane Functionalized Carbon Dots and Their Cross-Linked Flexible Silicone Rubbers for Color Conversion and Encapsulation of White Leds. *ACS Appl. Mater. Interfaces* **2016**, *8*, 9961-9968.

29. Wang, Y.; Wang, K.; Han, Z.; Yin, Z.; Zhou, C.; Du, F.; Zhou, S.; Chen, P.; Xie, Z., High Color Rendering Index Trichromatic White and Red Leds Prepared from Silane-Functionalized Carbon Dots. *Journal of Materials Chemistry C* **2017**, *5*, 9629-9637.

30. Corricelli, M., et al., Gisaxs and Giwaxs Study on Self-Assembling Processes of Nanoparticle Based Superlattices. *CrystEngComm* **2014**, *16*, 9482-9492.

31. Nguyen, V.; Si, J.; Yan, L.; Hou, X., Electron–Hole Recombination Dynamics in Carbon Nanodots. *Carbon* **2015**, *95*, 659-663.

32. Zhang, X., et al., Color-Switchable Electroluminescence of Carbon Dot Light-Emitting Diodes. *ACS Nano* **2013**, *7*, 11234-11241.

33. Zhu, S.; Song, Y.; Zhao, X.; Shao, J.; Zhang, J.; Yang, B., The Photoluminescence Mechanism in Carbon Dots (Graphene Quantum Dots, Carbon Nanodots, and Polymer Dots): Current State and Future Perspective. *Nano Research* **2015**, *8*, 355-381.

34. Zhang, Y.; Wang, Y.; Feng, X.; Zhang, F.; Yang, Y.; Liu, X., Effect of Reaction Temperature on Structure and Fluorescence Properties of Nitrogen-Doped Carbon Dots. *Appl. Surf. Sci.* **2016**, *387*, 1236-1246.

35. Zhu, S.; Zhao, X.; Song, Y.; Lu, S.; Yang, B., Beyond Bottom-up Carbon Nanodots: Citric-Acid Derived Organic Molecules. *Nano Today* **2016**, *11*, 128-132.

36. Sharma, A.; Gadly, T.; Gupta, A.; Ballal, A.; Ghosh, S. K.; Kumbhakar, M., Origin of Excitation Dependent Fluorescence in Carbon Nanodots. *J. Phys. Chem. Lett.* **2016**, *7*, 3695-3702.

37. Sharma, A.; Gadly, T.; Neogy, S.; Ghosh, S. K.; Kumbhakar, M., Addition to "Molecular Origin and Self-Assembly of Fluorescent Carbon Nanodots in Polar Solvents". *J. Phys. Chem. Lett.* **2017**, 5861-5864.

38. Panniello, A.; Binetti, E.; Ingrosso, C.; Curri, M. L.; Agostiano, A.; Tommasi, R.; Striccoli, M., Semiconductor Nanocrystals Dispersed in Imidazolium-Based Ionic Liquids: A Spectroscopic and Morphological Investigation. *Journal of Nanoparticle Research* **2013**, *15*, 1-14.

39. Wyszecki, G.; Stiles, W. S., *Color Science: Concepts and Methods, Quantitative Data and Formulae, 2nd Edition*, 2nd ed.; Wiley-VCH: New York, 1982, p 968.

40. Ingrosso, C.; Panniello, A.; Comparelli, R.; Curri, M. L.; Striccoli, M., Colloidal Inorganic Nanocrystal Based Nanocomposites: Functional Materials for Micro and Nanofabrication. *Materials* **2010**, *3*, 1316-1352.

TOC GRAPHIC

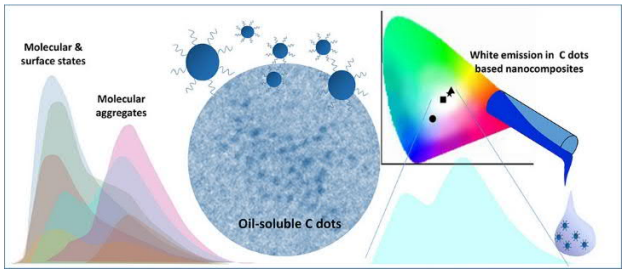
Molecular &
surface states
Molecular
aggregates
Oil-soluble C dots
White emission in C dots
based nanocomposites